



Brake Strategy Analysis for Industrial Normal-closed Brake Based on Rotational Inertia Test and Simulation

Yuantao Sun*, Kaige Chen, Qing Zhang, Xianrong Qin & Jianjie Zhang

School of Mechanical Engineering, Tongji University, No.4800,
Caoan Road, Shanghai, 201804, China

*E-mail: sun1979@sina.com

Abstract. Industrial brakes pose the dilemma of weighing brake capability against brake impact since the brake torque cannot be adjusted. On the one hand, the brake torque may be insufficient to stop the movement within a limited distance or parking position. On the other hand, the brake torque may be so high it can damage the transmission chain. In this study, the traditional brake strategy and the field oriented control (FOC) brake strategy were compared through simulation and a rotational inertia test. The influence of the rated brake torque and the open-closed ratio were obtained. Based on the test and simulation results, a semi-empirical formula that defines the relationship between relative brake capability and open-closed ratio was developed. Additional simulations were performed to analyze the performance of the brake in a flexible transmission chain. As an industrial application example, the benefits and the cost of a 'smart brake' based on the FOC brake strategy were analyzed. The results indicate that the equivalent brake torque with the FOC brake strategy is a function of the real-time controllable input and open-closed ratio, which can be conducted during the braking procedure. This can be an efficient way to solve the above problems.

Keywords: *brake impact; FOC brake strategy; industrial brake; normal-closed electromagnetic brake; rotational inertia test.*

1 Introduction

Large machinery such as port cranes have large mass and a large-scale structure, while the operational mechanism has to load and unload cargo frequently and rapidly. In the process of cargo handling, industry brakes are used to consume the kinetic energy of the cargo and to stabilize it at a suitable height.

The traditional braking approach is that a constant braking force, which can increase the security of the system, is applied to the brake disc, and the friction between the brake disc and the braking object reaches the preset braking force to stop the movement [1,2]. This braking approach can indeed accomplish the braking process, however, the large inertia of the braking object can result in a

huge impact, which may damage the weakest link in the chain of transmission [3]. In addition, the braking impact will transmit to the whole structure of the machine through the transmission system. Consequently, a series of adverse consequences can occur. The operational mechanism may shake violently; driving comfort will be influenced, which can make the driver get tired easily [4,5]; and, finally, excessive impact may directly lead to damage to the operational mechanism and even the whole structure. Figure 1 shows a smashed gearbox that was broken in the brake process. The smashed gearbox is called a jack-up gearbox with a 1:8000 ratio, developed for offshore platforms, which was destroyed during a test running of the emergency brake process. The brake impact destroyed 3 of its 76 gearboxes since the brake torque was too high for this application.



Figure 1 Smashed gearbox of a jack-up device.

In order to reduce the disadvantages of the traditional braking process in large machinery, an improvement that can relieve the braking impact and mitigate unwanted side effects of the braking process is essential.

In previous researches and applications, most attention was paid to the braking moment. It is considered that a larger braking moment is more beneficial to stop the movement of the equipment. In some technical specifications, the brake selection is determined by the braking moment, which is calculated based on the braking time and the inertia of the braking object. Moreover, the heat quantity converted from the kinetic energy of the braking object should be checked in order to avoid failure of the brakes caused by overheating. Hence, some researches have focused on heat attenuation of materials for braking [6-12], Grzes, *et al.* [13] developed a model of a disk brake to study the temperature at the discrete contact between two rough surfaces and studied two approaches of calculation of the flash temperature. However, the system dynamic of the

braking process was not taken into consideration and the braking impact on the transmission link was not analyzed either.

Researches with an engineering background are mostly found in robot control and vehicle engineering. Seungbok, *et al.* [14-16] studied the design and optimization of magneto-rheological brakes in several engineering applications and discussed the influence of different parameters, such as weight, brake torque, etc. in these applications. Gáspár, *et al.* [17,18] have proposed several brake strategies and analyzed their performances in vehicle automation. He, *et al.* in [19-21] discuss the dynamics of an integrated system with different types of brakes and their application in vehicle engineering. Hirata, *et al.* [22-24] focused on servo-brake control issues in several kinds of robot motion control. Picasso, *et al.* [25] considered braking control problems for railway vehicles and proposed a novel distributed braking control algorithm based on preview control theory.

Antilock brake systems (ABS) are widely applied in the automobile industry, since it can keep the rotational wheel from locking and, consequently, guarantee maneuverability by discontinuously braking in emergency conditions [26]. The essence of ABS is to constrain the slip ratio of the wheel within a certain range [27,28]. It guarantees both the shortest brake distance and the best steering handling stability, therefore in the automobile industry many researches on brake strategies have been conducted from the viewpoint of system dynamics [29,30].

Inspired by ABS, a new smart brake strategy for industry brakes is proposed. If the condition of the brake is not always closed and the braking force is alternately on and off, there will be a time period during which the brake disc is not in contact with the braking object. As a result, the brake can avoid the impact generated by the kinetic energy from the braking object. Moreover, the braking time is adjustable by controlling the frequency of the open and closed condition of the brake. Thus, the braking process can be gentler. Such a process is similar to an ABS in vehicles. However, this process applied to industrial brakes is essentially different from that applied in ABS. In ABS, it is critical to control the wheel slip ratio to stay within a stable range, whereas the goal of using a brake in the industrial field is to keep the safety of the machinery in such a way that the kinetic energy of the braking object can be dissipated during the braking time. There is no influence of the slip ratio on the braking process of an industrial brake.

Based on this novel smart braking strategy, the feasibility of a rapidly open-closed brake process was verified. Firstly, a typical dynamic model of a transmission system was constructed. The braking impact was analyzed on the

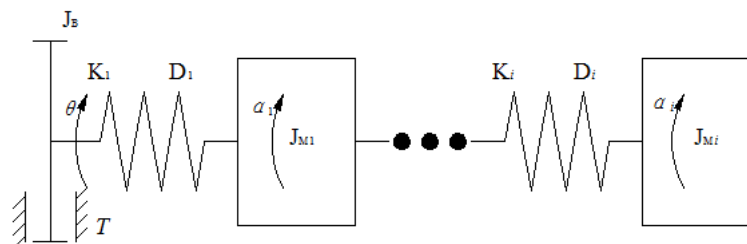
dynamic model and the feasibility was verified in theory. Then, based on the theoretical analysis, an inertia test stand was implemented. The deceleration values under different open-closed frequencies were tested and compared with the theoretical results. Both the theoretical and the experimental results indicated that the proposed smart braking strategy can reduce the impact on the transmission system in view of brake process safety.

2 Dynamic Model of Transmission Chain During Brake Process

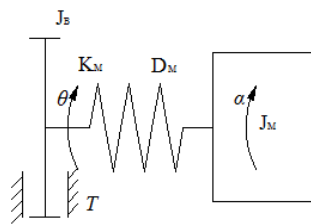
2.1 Dynamic Model of Transmission Chain

The transmission chain is usually an assembly of several components to achieve the operational tasks. Every component has its own mass, stiffness and damping characteristics. As shown in Figure 2(a), the system was modeled as an assembly of a brake, whose moment of inertia is J_B , and other components, whose moments of inertia are J_i . The connections with neighboring components consist of rotational springs with stiffness K_i and damping D_i . Deformation only happens in the connections in the system.

Similar to the idea in the finite element method of super-elements [31], the DOFs of mechanisms on the transmission chain condensates to a single part, denoted as JM, while the entire stiffness and damping are denoted as KM and DM. A simplified diagram is shown in Figure 2(b).



(a) Finite DOF transmission chain



(b) Condensation model with all flexibility

Figure 2 Diagram of the dynamic model of a flexible transmission chain.

The dynamic equation of the system is as follows:

$$\begin{bmatrix} J_B & \\ & J_M \end{bmatrix} \cdot \ddot{\mathbf{X}} + \begin{bmatrix} D_{\text{inter}} & -D_{\text{inter}} \\ -D_{\text{inter}} & D_{\text{inter}} \end{bmatrix} \cdot \dot{\mathbf{X}} + \begin{bmatrix} -K_{\text{inter}} & K_{\text{inter}} \\ K_{\text{inter}} & -K_{\text{inter}} \end{bmatrix} \cdot \mathbf{X} = \begin{Bmatrix} -T \\ 0 \end{Bmatrix} \quad (1)$$

where J_B denotes the moment of the brake and J_M is the moment of the mechanism; D_{inter} is the damping coefficient at the interface, which is a scalar; K_{inter} denotes the stiffness coefficient at the interface; T is the brake torque; and $\mathbf{X} = \{\theta, \alpha\}^T$ is the position vector of the system.

2.2 Brake Strategy

For an electromagnetic normally-closed brake, there are two common brake strategies:

1. Traditional brake strategy

The brake torque of a normally-closed brake with a traditional brake strategy is shown in Eq. (2), as widely applied in industry:

$$T_n = \begin{cases} 0 & (F_b == \text{OPEN}) \\ T_{\text{rated}} & (F_b == \text{CLOSE}) \end{cases} \quad (2)$$

where T_n denotes the brake torque with the traditional brake strategy; T_{rated} is the rated torque of the brake; F_b represents the control signal flag for the brake action.

In this case, the brake has either ‘OPEN’ or ‘CLOSED’ status, which means that the brake torque can be either zero or the rated value. This strategy can be regarded as ‘rigid’, because the brake torque cannot be adjusted during the braking process.

2. Fast open-closed brake strategy

In order to adjust the brake torque during the braking process, a fast open-closed brake strategy is proposed. The variation of the torque is shown in Eq. (3):

$$T_{\text{FOC}}(\text{rat}) = \begin{cases} 0 & F_b == \text{OPEN} \\ T_{\text{rated}} & (F_b == \text{CLOSE}) \& (n \cdot t_0 < t \leq n \cdot t_0 + \text{rat} \cdot t_0) \\ 0 & (F_b == \text{CLOSE}) \& (n \cdot t_0 + \text{rat} \cdot t_0 < t \leq (n+1) \cdot t_0) \end{cases} \quad (3)$$

where t_0 is the period of a single open and closed cycle; $\text{rat} = t_{\text{close}}/t_0$ denotes the ratio of the closed time against the period; n represents the integer to determine the cycle.

A diagram of these two strategies is shown in Figure 3.

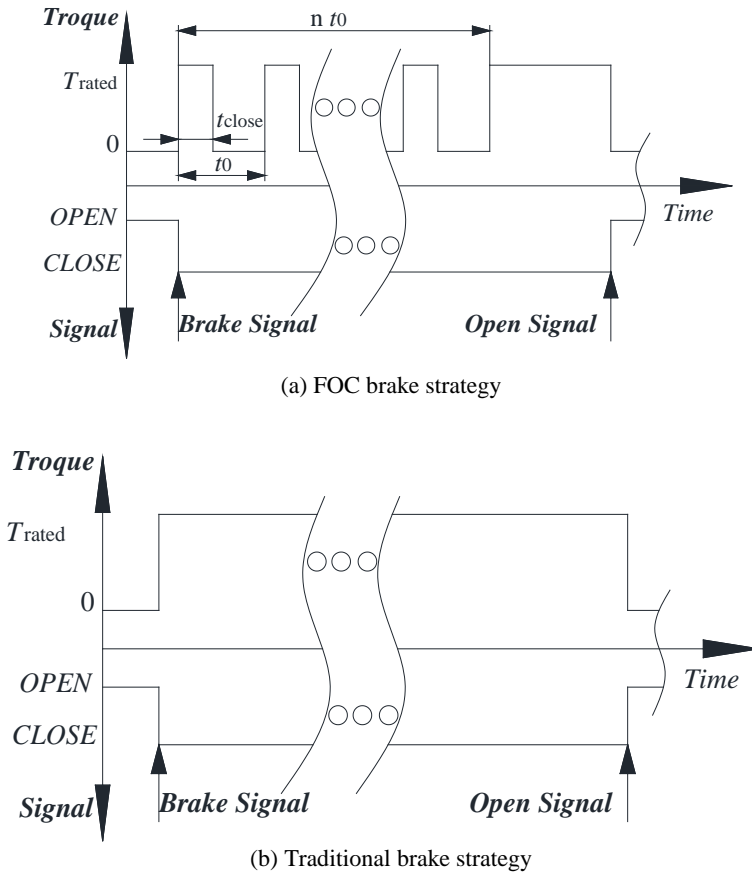


Figure 3 The trajectories of the two brake strategies.

For the fast open-closed strategy, the equivalent brake torque is regarded as the integration of the current brake torque, as shown in Eq. (4).

$$T_{\text{FOC}}(\text{rat}) = \begin{cases} 0 & (F_b = \text{OPEN}) \\ \int \begin{cases} T_{\text{rated}} & (n \cdot t_0 < t \\ \leq n \cdot t_0 + \text{rat} \cdot t_0) \\ 0 & (n \cdot t_0 + \text{rat} \cdot t_0 < t \\ \leq (n+1) \cdot t_0) \end{cases} dt & (F_b = \text{CLOSE}) \end{cases} = \begin{cases} 0 & (F_b = \text{OPEN}) \\ \text{rat} \cdot T_{\text{rated}} & (F_b = \text{CLOSE}) \end{cases} \quad (4)$$

By adjusting the ratio of the closed time against the period, the brake torque varies linearly. At the same time, it is clear that if the ratio is equal to one, the

traditional brake strategy is described. In other words, the traditional brake strategy is a special case of the FOC brake strategy.

3 Test, Results and Discussion

3.1 Structure of the Rotational Inertia Test Bench

The aim of the brake is to stop the motion and consume the kinetic energy of a mechanism. Accordingly, to test the performance of a brake, the kinematic energy is the most essential concern. A rotational inertia test bench is commonly used to test the performance of a brake system. As shown in Figure 4, the rotational inertia test bench consists of: (1) an encoder, which records the time history of the angular velocity; (2) a motor, which is the driver of the test bench; (3) an inertial load, which is the moment of inertia that represents the actual payload; (4) a brake, which is the brake to be tested.

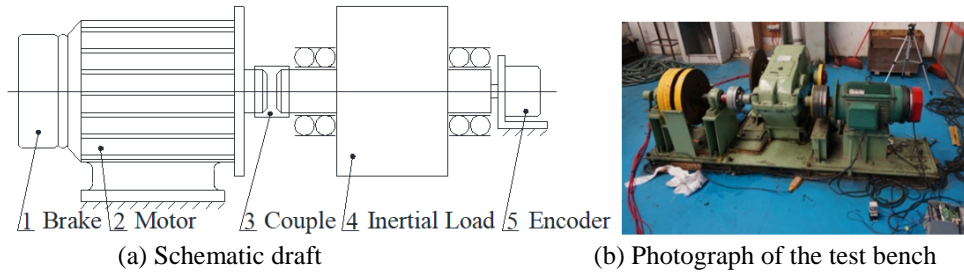


Figure 4 The rotational inertia test bench used in the test.

In application, the moment of inertia is known as a constant, J , which is designed according to the requirements of different products; the initial angular velocity, $\dot{\alpha}_0$, is known and depends on the trajectory of the motor. Using a linear approach, the two most important parameters are calculated with Eqs. (5) and (6).

$$T = J \cdot \frac{d\dot{\alpha}}{dt} \quad (5)$$

$$E_k = \frac{1}{2} J \cdot \dot{\alpha}^2 \quad (6)$$

where J is the moment of the inertial load; $\dot{\alpha}$ denotes the angular velocity of the test bench; T represents the brake torque; and E_k is the kinematic energy of the system.

The rotational inertia test bench (shown in Figure 4(b)) is discussed below and its basic parameters are listed in Table 1.

Table 1 Parameters of the test bench.

$J(\text{kg m}^2)$	$\dot{\alpha}_0$ (rad/s)	$T_{\text{rated}} (\text{N}\cdot\text{m})$	t_0 (s)	rat
5.59	83.78	187.32	0.250	0.28-0.56

The test was performed at nine ratios and five times per ratio. The time history of the angular velocity was recorded. The results are analyzed in the following section.

3.2 Test Results

The main concern in the braking process is the angular acceleration. The initial uniform rotation and the situation after the initial load has completely been stopped are not of interest to this research.

After the treatment, the time history is regarded as a linear relationship. The slope of the curve is the angular acceleration and the intercept is the initial angular velocity. Thus, the velocity curves are fitted according to the least square method to a straight line as shown in Eq. (7). Figure 8 shows the time histories of the angular velocity and its fitting curves with different brake ratios (the superscript t stands for 'test'):

$$\dot{\alpha} = A1 \cdot t + A2 \quad (7)$$

where $A1$ and $A2$ are the linearized coefficient of the angular velocity fitting curve, $A1$ represents the angular acceleration, and $A2$ represents the initial angular velocity; and t is time.

3.3 Error Analysis between Test and Simulation

To check the dynamic model of the transmission chain shown in Eq. (3), the same inputs listed in Table 1 are introduced into the model.

As can be seen in Figures 7 and 8, the coefficients of $A1$ and $A2$ in Eq. (7) for both the test and the simulation are listed in Table 2.

As can be seen in Table 2, there is an error between the test data and the simulation data. Since the error of $A2$ is comparably small and it is of less importance to the performance of the brake, the following discussion focuses on angular acceleration $A1$. As shown in Eq. (1), it can be inferred that angular acceleration $A1$ is a function of ratio rat and the rated constant of T_{rated}/J . Normally, for a particular test bench, the moment J always remains the same.

Thus, the system error most likely came from the rated brake torque and the open-closed ratio.

As shown in Figure 2(b), the brake torque is from a pre-tensioned spring. The stiffness of the spring and the initial tension of different brakes may vary. Therefore, the actual rated brake torque is as expressed in Eq. (8).

$$T_{\text{rated}}^t = k_a \cdot T_{\text{rated}} \quad (8)$$

where k_a is a positive amplifier of the rated brake torque; T_{rated} is the standard brake torque.

Table 2 Coefficients of the linearized curve of the angular velocity.

rat	A1 _t	A2 _t	A1 _s	A2 _s
0.28	-2.68	84.9	-2.32	83.6
0.32	-3.8	80.7	-4.67	83.3
0.36	-6.04	80.4	-7.46	83.1
0.38	-12.2	78	-9.32	83
0.44	-11.7	79.7	-14	82.8
0.46	-20.7	79.8	-16.1	82.8
0.48	-15	80.4	-17.5	82.4
0.52	-20.3	81.8	-18.6	78.2
0.56	-27	83.6	-18.3	72.3
0.28	-2.68	84.9	-2.32	83.6
0.32	-3.8	80.7	-4.67	83.3

With a linear approach, the relationship between the angular acceleration and the brake torque implies that:

$$\ddot{\alpha} = T_{\text{rated}} / J \cdot \text{rat} \quad (9)$$

When $\text{rat} = 1$, the amplifier k_I can be calculated by simultaneously solving Eqs. (8) and (9), as shown in Eq. (10):

$$k_I = \ddot{\alpha}_t / \ddot{\alpha}_{\text{rated}} = A1_t(\text{rat} = 1) / A1_s(\text{rat} = 1) \quad (10)$$

where $A1_t(\text{rat} = 1)$ and $A1_s(\text{rat} = 1)$ represent the values based on the test and the simulation when the open-closed ratio is equal to one.

Another possible source of the error is from an error in the actual open-closed ratio. Since the ratio is defined as $\text{rat} = t_{\text{close}}/t_0$, the error may exist in both the period of a single cycle and the closed time, as shown in Eq. (11):

$$\begin{cases} t_0^t = k_p \cdot t_0^s \\ t_{\text{close}}^t = k_d t_{\text{close}}^s{}^2 + k_1 t_{\text{close}}^s + \delta t \end{cases} \quad (11)$$

where the superscript s and t represent ‘standard’ and ‘test’, respectively; k_p is the amplifier of the single error in the open-closed cycle; k_d and k_1 are the possible quadratic coefficients of the error in closed time; δt is the delay of the closed time.

Thus, the error in the open-closed ratio is:

$$\begin{aligned} rat^t &= \frac{t_{close}^t}{t_0^t} = \frac{k_d}{k_p \cdot t_0^s} \cdot t_{close}^s{}^2 + \frac{k_1}{k_p \cdot t_0^s} \cdot t_{close}^s + \frac{\delta t}{k_p \cdot t_0^s} \\ &= k_1 \cdot t_{close}^s{}^2 + k_2 \cdot t_{close}^s + k_3 \end{aligned} \quad (12)$$

With the linear assumption shown in Eq. (9), the error of the angular acceleration is a function of the open-closed ratio. Taking Eq. (12) into account, the error can be defined as follows:

$$err_{\ddot{\alpha}} = \ddot{\alpha}_t - \ddot{\alpha}_s = \frac{k_a \cdot T_{rated}}{J} \left(\frac{k_d}{k_p \cdot t_0^s} \cdot t_{close}^s{}^2 + \frac{k_1}{k_p \cdot t_0^s} \cdot t_{close}^s + \frac{\delta t}{k_p \cdot t_0^s} \right) - \frac{k_a \cdot T_{rated}}{J \cdot t_0^s} \cdot t_{close}^s \quad (13)$$

To determine the coefficients shown in Eq. (13), Eq. (13) is simplified into the following form:

$$err_{\ddot{\alpha}} = \ddot{\alpha}_t - \ddot{\alpha}_s = U1 \cdot (t_{close}^s)^2 + U2 \cdot t_{close}^s + U3 \quad (14)$$

where U1, U2 and U3 are the coefficients of the polynomial, which are defined according to the quadratic least square method curve fitting of the result of the test data and the simulation data. Finally, the coefficients k_1 , k_2 and k_3 shown in Eq. (12) are calculated.

3.4 Relationship between Open-closed Ratio and Angular Acceleration

Table 3 lists the polynomial coefficient of error estimation between the test data and the simulation data. As shown in Table 3, the coefficient k_a , which represents the rated torque, is 1.16 times greater than its nominal torque; k_1 , k_2 and k_3 indicate that the error is close to a linear curve.

Table 3 Coefficients of the polynomial of the error estimation between test and simulation.

Coefficient	Value	Coefficient	Value
k_a	1.16	U1	-1.44×10^{-2}
k_1	-3.71×10^{-4}	U2	1.25
k_2	1.03	U3	65.82
k_3	0.7		

According to Eqs. (11) and (12), the actual open-closed ratio can be corrected by the coefficients in Table 3. As shown in Figure 9, the relationship between the corrected open-closed ratio and the angular deceleration is compared with the test data.

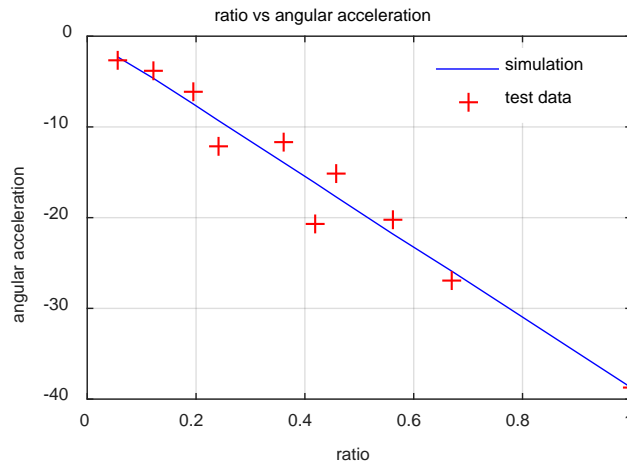


Figure 5 Angular deceleration vs. the open-close ratio.

As shown in Figure 5, the relationships between the open-closed ratio and the angular deceleration correspond to one another and approach a straight line. With the increase of the open-closed ratio, the deceleration increases.

To adapt the engineering application, the relationship between the open-closed ratio and the normalized angular acceleration is shown in Eq. (15) according to the quadratic least square method.

$$\gamma = B1 \cdot rat + B2 \tag{15}$$

where, $\gamma = \ddot{\alpha} / \ddot{\alpha}_{rated}^t$ is the normalized angular acceleration and $\ddot{\alpha}_{rated}^t$ is the angular acceleration from the test data when the open-closed ratio is equal to one; $B1 = -9.998E-1$ and $B2 = 4.000E-4$ are the coefficients of the fitting curve. It shows that the relative angular acceleration is close to the open-closed ratio. Thus, it can be inferred that the equivalent brake torque is the rated torque multiplied with the ratio.

3.5 Analysis of Brake Impact vs Ratio

The angles at the brake disc side θ or the inertial load side α are different due to the flexibility of the transmission chain. The deformation between these two angles δ is an index of the brake impact:

$$\delta = \alpha - \theta \quad (16)$$

where δ is the angular deformation of the transmission chain; θ is the rotation angle at the brake disc side; and α is the rotation angle at the inertial load side.

Figure 6 shows the time histories of the angular deformation during braking with different open-closed ratios.

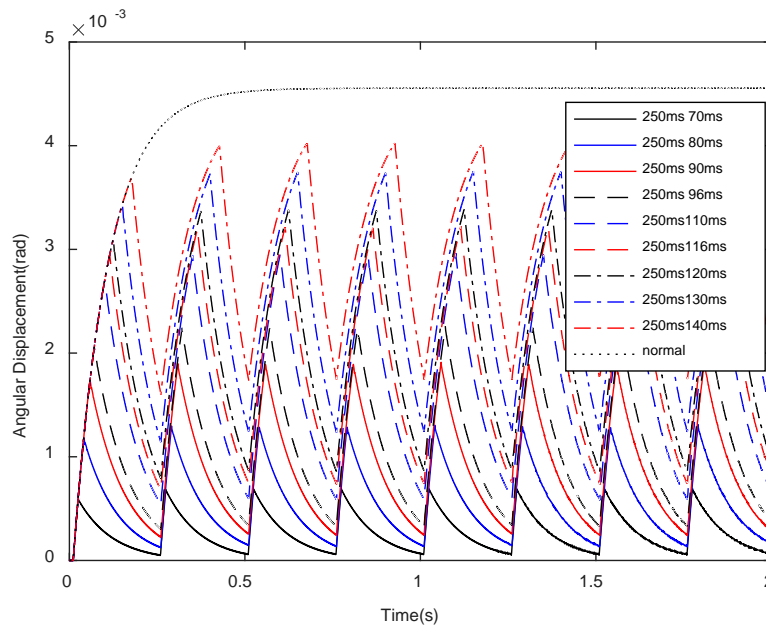


Figure 6 Time histories of the differential between two angles $\delta = \alpha - \theta$.

Figure 6 indicates that during the braking process (with a constant deceleration), the differential decreases with the decrease of the open-closed ratio and when the ratio is equal to one, the differential reaches its maximum. At uniform to the maximum differential angle and when $rat = 1$, the relationship between the open-closed ratio and uniform maximum angular deformation is shown in Figure 7.

As can be seen in Figure 7, the relative maximum angular deformation increases with the increase of the open-closed ratio. When the ratio exceeds 0.5, the slope of the curve shown in Figure 7 is smaller than one. This indicates that the brake impact declines as the open-closed ratio increases, especially when the ratio is close to one.

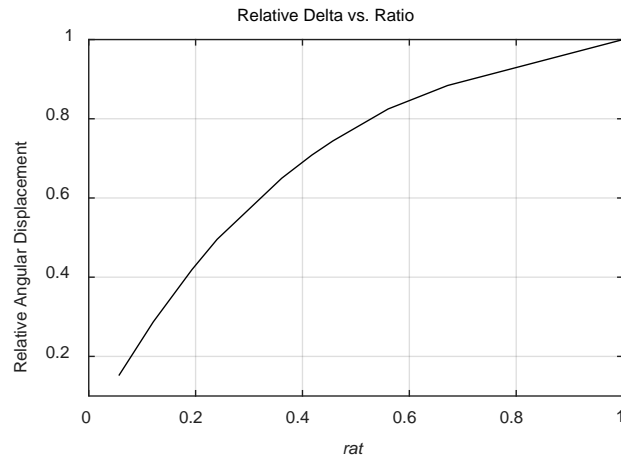


Figure 7 Relationship between open-closed ratio and uniform maximum angular deformation.

4 Application: Smart Brake

4.1 Trajectory of the Smart Brake

As discussed in the previous section, the angular deceleration is a function of the input ratio of the FOC brake strategy. Thus, it is possible to operate the brake torque during the braking process. This is the principle of the so-called smart brake [3-5]. The FOC brake strategy can certainly reduce the brake impact and increase the brake distance compared with the traditional strategy. As shown in Figure 8, the maximum angular deformation with a smart brake strategy is obviously smaller than with a traditional brake strategy.

The smart brake works according to the diagram shown in Figure 4(a). Normally, the rated brake torque can be set at a higher value (1.3 times for example) than a traditional one. To avoid too large a brake impact, the FOC strategy is used to reduce the brake impact during the deceleration process. Figure 8 shows a comparison between the smart brake system and the traditional brake system.

As shown in Figure 8, the traditional brake system can only output a constant brake torque in accordance with the brake signal. The rated brake torque is set by balancing the brake distance and the brake impact and the parking requirements. In industrial applications, the brake torque should be capable of stopping the motion within a limited distance or time, and the transmission

chain is checked according to the torque. At the same time, the brake torque should be greater and better in a parking situation.

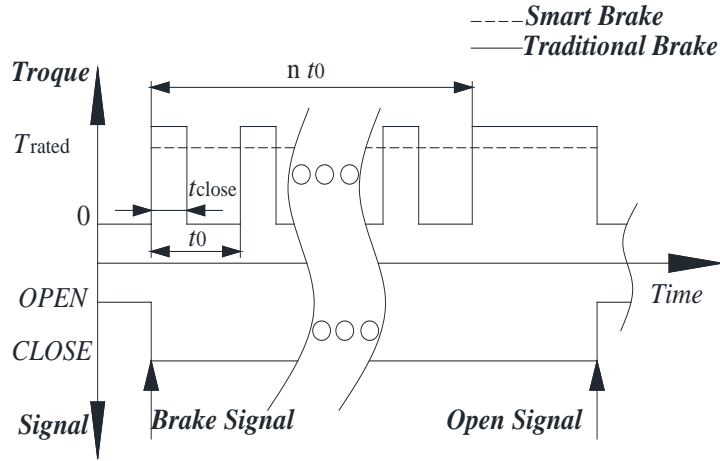


Figure 8 Comparison of a smart brake system and a traditional brake system.

Thus, the principle of the trajectory design of the smart brake should be as follows:

1. During the deceleration process, the equivalent brake torque is the same as that of the traditional brake.
2. In a parking situation, the brake torque is greater than the rated brake torque of the traditional brake. This principle is expressed as follows:

$$T_{\text{smart}}(\text{rat}) = \begin{cases} A_{\text{smart}} \cdot T_{\text{rated}} \cdot \text{rat} \approx T_{\text{rated}} & (\text{during deceleration}) \\ A_{\text{smart}} \cdot T_{\text{rated}} & (\text{parking situation}) \end{cases} \quad (17)$$

where the T_{smart} is the equivalent brake torque of the smart brake; T_{rated} is the rated brake torque of the traditional brake strategy; A_{smart} is the amplifier of the rated brake torque of the smart brake, which is a constant according to the designed brake characteristics; rat is the open-closed ratio of the FOC brake strategy.

4.2 Performance Analysis

As shown in Eq. (17), the most attractive benefits of the smart brake are that: (a) the equivalent brake torque can be adjusted during operation, and (b) the rated brake torque is amplified when compared with the traditional one.

For example, the response of the transmission chain when $A_{\text{smart}} = 1.3$, $rat = 0.8$ is introduced into the brake strategy is shown in Figure 9. In order to discuss the influence of the brake strategy and the amplifier, three situations are considered: (a) the traditional brake strategy with a rated torque, which indicates that: $A_{\text{smart}} = 1.0$ and $rat = 1.0$; (b) the traditional brake strategy with an amplified torque, which indicates that: $A_{\text{smart}} = 1.3$ and $rat = 1.0$; (c) the smart brake strategy with an amplified torque, which indicates that $A_{\text{smart}} = 1.3$ and $rat = 0.8$. The simulation results are shown in Figure 9.

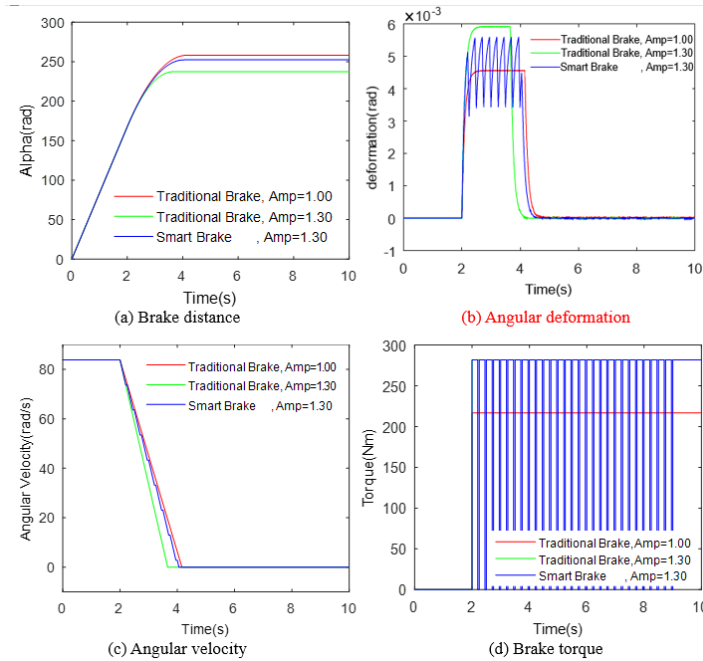


Figure 9 Time history of the response of the transmission chain.

By comparing the curves, the parameters of these three trajectories are listed in Table 4.

1. The benefits are obvious, i.e.:
 - a. The smart brake has a higher final brake torque, which is the most important characteristic of the brake in a parking situation;
 - b. The brake impact is relatively small compared with the traditional brake with the same final brake torque;
 - c. The brake distance is comparatively small, which is not as great as the traditional brake without amplifier.

Hence, the smart brake is the most flexible way to solve the problem of weighing the brake impact against the brake torque.

2. The cost

On the other hand, however, the benefits of the smart brake strategy come with the cost of an increase in brake distance. To analyze the performance of a brake system, the two most essential factors are: (a) the brake distance; (b) the brake impact during the braking process. To discuss these two factors, the following normalized values are used:

$$\begin{cases} \gamma_{ipt} = \frac{\max(\delta(rat = 1)) - \max(\delta(rat))}{\max(\delta(rat = 1))} \\ \gamma_{dis} = \frac{\max(\alpha(rat)) - \max(\alpha(rat = 1))}{\max(\alpha(rat = 1))} \end{cases} \quad (18)$$

where γ_{ipt} and γ_{dis} are the relative decrease of the angular deformation and the relative increase of the brake distance, which are the normalized factors; δ is the angular deformation, which indicates the brake impact; α is the brake distance at the inertial load side; and rat is the open-closed ratio of the FOC strategy.

According to the simulation results, the curves of these two factors for different open-closed ratios are shown in Figure 10.

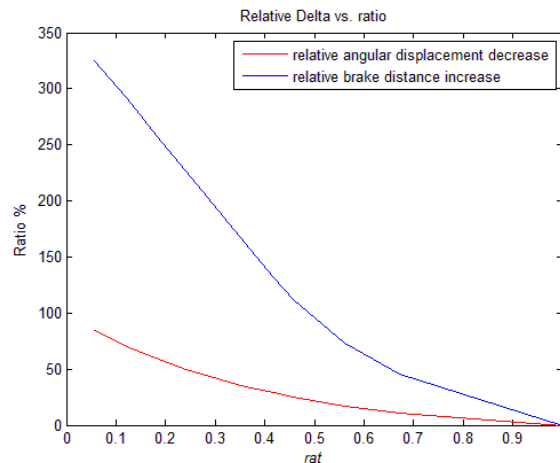


Figure 10 Ratio of decrease in angular deformation and increase in brake distance.

As shown in Figure 10, the blue curve represents the increase of brake distance for different open-closed ratios and the red curve indicates the decrease of brake impact. When the ratio is equal to one, there is no decrease in angular deformation or increase in brake distance. With the FOC strategy, the increase

of the brake distance is always greater than the decrease of the brake impact. This is the cost of the FOC brake strategy in normally-closed brakes.

5 Conclusions

With all the dimensions discussed above, the conclusion can be drawn that in accordance with different input ratios of the novel FOC brake strategy, the kinematic characteristics in the transmission chain vary. The relationship between the open-closed ratio and the deceleration has a linear trend, and the dynamic response of the maximum deformation in the transmission chain decreases with the decrease of the open-closed ratio.

The cost of the smaller brake impact is an increase in brake distance. With a proper design, in most cases, the increase is relatively small and harmless. The smart brake system has good flexibility when facing different kinds of situations, so it is a possible method to get out of the dilemma of weighing brake impact against brake capability.

Acknowledgements

This work was supported by the National Key Research and Development Program of China (No. 2018YFC0808902). The test mentioned in this article was developed by the ZPMC – Jiangxi Huawu Brake Co. Ltd.

References

- [1] Du, Y.C, Qin, C.A. & You, S.X., *Efficient Coordinated Control of Regenerative Braking with Pneumatic Anti-lock Braking for Hybrid Electric Vehicle*, Science China-Technological Sciences, **60**(3), pp. 1-13, 2017.
- [2] Peng, H., Wang, J., Shen, W., Shi, D. & Huang, Y., *Controllable Regenerative Braking Process for Hybrid Battery-Ultracapacitor Electric Drive Systems*, IET Power Electronics, **11**(15), pp. 2507-2514, 2018.
- [3] Yin, G. & Jin, X.J., *Cooperative Control of Regenerative Braking and Antilock Braking for a Hybrid Electric Vehicle*, J. Mathematical Problems in Engineering, **2013**(4), pp. 1-9, 2013.
- [4] Dunjian, F., *The Quayside Container Cranes*, Hubei Science and Technology Press, 2007.
- [5] Yuantao, S. & Pincai, C., *The Application of the Smart Brake in Anti-Block System in Self-Driving Trolley On Bridge Crane*, Port Operation, **3**, pp. 10-11, 2013.
- [6] Shin, M.W., Kim, J.W, Joo, B.S. & Jang, H., *Wear and Friction-induced Vibration of Brake Friction Materials with Different Weight Average*

- Molar Mass Phenolic Resins*, Tribology Letters, **58**(1), 2015. DOI: 10.1007/s11249-015-0486-5.
- [7] Lee, S.M., Shin, M.W. & Jang, H., *Friction-Induced Intermittent Motion Affected by Surface Roughness of Brake Friction Materials*, Wear, **308**(1-2), pp. 29-34, 2013.
- [8] Park, C.W., Shin, M.W. & Jang, H., *Friction-induced Stick-Slip Intensified by Corrosion of Gray Iron Brake Disc*, Wear, **309**(1-2), pp. 89-95, 2014.
- [9] Rhee, S.K., Jacko, M.G. & Tsang, P.H.S., *The Role of Friction Film in Friction, Wear and Noise of Automotive Brakes*, Wear, **146**(1), pp. 89-97, 1991.
- [10] Rhee, S.K., Tsang, P.H.S. & Wang, Y.S., *Friction-Induced Noise and Vibration of Disc Brakes*, Wear, **133**(1) pp. 39-45, 1989.
- [11] Jacko, M.G., Tsang, P.H.S. & Rhee, S.K., *Wear Debris Compaction and Friction Film Formation of Polymer Composites*, Wear, **133**(1), pp. 23-38, 1989.
- [12] Labdi, A. & Bouchetara, M., *The Application of the Design of Experiments Approach in Thermal and Structural Calculation of a Brake Disk*, Journal of the Chinese Society of Mechanical Engineers, **39**, pp. 491-499, 2018.
- [13] Grzes, P., *Finite Element Solution of the Three-Dimensional System of Equations of Heat Dynamics of Friction and Wear during Single Braking*, Advances in Mechanical Engineering, **10**(11), pp. 1-15, 2018.
- [14] Sohn, J.W., Jeon, J., Nguyen, Q.H. & Choi, S.-B., *Optimal Design of Disc-Type Magneto-Rheological Brake for Mid-Sized Motorcycle: Experimental Evaluation*, Smart Materials and Structures, **24**(8), 085009, 2015. DOI: 10.1088/0964-1726/24/8/085009.
- [15] Nguyen, Q.H., Lang, V.T. & Choi, S.B., *Optimal Design and Selection of Magneto-Rheological Brake Types Based on Braking Torque and Mass*, Smart Materials and Structures, **24**(6), 067001, 2015. DOI: 10.1088/0964-1726/24/6/067001.
- [16] Nguyen, Q.H. & Choi, S.B., *Optimal Design of a Novel Hybrid MR Brake for Motorcycles Considering Axial and Radial Magnetic Flux*, Smart Materials and Structures, **21**(5), 055003, 2012. DOI: 10.1088/0964-1726/21/5/055003.
- [17] Gáspár, P., Szabo, Z. & Bokor, J., *Brake Control Using an Estimation of the Wheel-Rail Friction Coefficient*, 2007 European Control Conference, ECC, pp. 362-367, 2007.
- [18] Németh, B. & Gáspár, P., *Analysis and Control of Nonlinear Actuator Dynamics Based On the Sum of Squares Programming Method*, IEEE/ASME International Conference on Advanced Intelligent Mechatronics, pp. 233-238, 2014.

- [19] Hu, D. & He, R., *Safety Design and Matching Analysis of Electronic Hydraulic Brake System*, Nongye Gongcheng Xuebao/Transactions of the Chinese Society of Agricultural Engineering, **31**(9), pp. 77-84, 2015.
- [20] He, R., Tang, B. & Zhao, Q., *Switching Control Strategy of Integrated Electromagnetic and Friction Brake System*, Jiangsu Daxue Xuebao (Ziran Kexue Ban)/Journal of Jiangsu University (Natural Science Edition), **36**(2), pp. 125-129, 2015.
- [21] He, R., Liu, X-J. & Liu, C-X., *Research Progress In Electromagnetic-Hydraulic Hybrid Brake Technology*, Zhongguo Gonglu Xuebao/China Journal of Highway and Transport, **27**(11), pp. 109-119, 2014.
- [22] Saida, M., Hirata, Y. & Kosuge, K., *Pose Estimation of Servo-Brake-Controlled Caster Units Arbitrarily Located on a Mobile Base*, IEEE International Conference on Intelligent Robots and Systems, pp. 3456-3462, 2014.
- [23] Hirata, Y., Kosuge, K. & Monacelli, E., *Power Steering and Force Display Controls for a Cycling Wheelchair Using Servo Brakes*, Proceedings – IEEE International Conference on Robotics and Automation, pp. 613-618, 2014.
- [24] Liu, Z., Zhang, M., Xu, J., Zhu, Y., Hirata, Y. & Kosuge, K., *A Passive Dance Robot with Active Coordination Capability*, IEEE International Conference on Mechatronics and Automation, IEEE ICMA, pp. 686-691, 2014.
- [25] Picasso, B., Caporale, D. & Colaneri, P., *Braking Control in Railway Vehicles: A Distributed Preview Approach*, IEEE Transactions on Automatic Control, **63**(1), pp. 189-195, 2018.
- [26] Sun, W., Zhang, J. & Liu, Z., *Two-Time-Scale Redesign for Antilock Braking Systems of Ground Vehicles*, IEEE Transactions on Industrial Electronics, **66**(6), pp. 4577-4586, 2019.
- [27] Penny, W.C.W. & Els P.S., *The Test and Simulation of ABS on Rough, Non-deformable Terrains*, Journal of Terra Mechanics, **67**, pp. 1-10, 2014.
- [28] Yin, D., Sun, N., Shan, D. & Hu, J.-S., *A Multiple Data Fusion Approach to Wheel Slip Control for Decentralized Electric Vehicles*, Energies, **10**(4), Article No. 461, pp.1-24, 2017.
- [29] Lu, L.Y., Lin, G.L. & Lin, C.Y., *Experiment of an ABS-type Control Strategy for Semi-Active Friction Isolation Systems*, Smart Structures & Systems, **8**(5), pp. 501-524, 2011.
- [30] Chao, C.Y., Yang, S.C. & Guo, Y.W., *The Brake Assist System of Automobile Overhaul Competence Analysis*, Advanced Materials Research, **301-303**(1), pp. 1464-1470, 2011.
- [31] Zeng, P., *Finite Element Analysis and Applications*, Tsinghua University Press, Springer, 2006.